J Solid State Electrochem (2010) 14:757–767
DOI 10.1007/s10008-009-0838-x

ORIGINAL PAPER

Influence of structural transformations over the electrochemical behavior of Ti anodic films grown in 0.1 M NaOH

Próspero Acevedo-Peña · Gerardo Vázquez · Dionisio Laverde · Julio E. Pedraza-Rosas · Ignacio González

Received: 29 January 2009 / Revised: 19 March 2009 / Accepted: 20 March 2009 / Published online: 30 April 2009

Abstract In this work, the structural transformation during the anodic growth of Ti oxide films and its influence on the resistive properties of the film are studied. The voltammetric characterization of Ti/0.1 M NaOH indicates that the oxide film composition depends on potential. Depending on the anodic switching potential, the oxide film can produce up to three cathodic peaks, and the peaks can be related to different Ti oxides. During the early stages of potentiostatic formation, the oxide film seems to have the same initial structure regardless of the film formation potential; however, after increasing growth time, the oxide structure depends on the formation potential. The evaluation of the resistive properties of Ti oxide films determined by electrochemical impedance spectroscopy shows that despite the chemical transformations within the film, there is a linear dependence between the capacitance of the Ti oxide film with formation potential.

P. Acevedo-Peña · D. Laverde · J. E. Pedraza-Rosas
Grupo de Investigaciones en Minerales Biohidrometalúrgia y Ambiente (GIMBA), Universidad Industrial de Santander (UIS),
Apdo. Postal 678,
Bucaramanga, Colombia

P. Acevedo-Peña · I. González (✉)
Departamento de Química, Universidad Autónoma Metropolitana, unidad Iztapalapa (UAM-I),
Apdo. Postal 55-534,
09340 Mexico, DF, Mexico
e-mail: igm@xanum.uam.mx

G. Vázquez
Departamento de Química, Centro de Investigación y Estudios Avanzados del I.P.N., (CINVESTAV-IPN),
Av. Instituto Politécnico Nacional 2508,
Col. San Pedro Zacatenco,
CP 07360 Mexico, DF, Mexico

Keywords Titanium oxide film · Structure transformation · Potentiostatic growth · Voltammetry · EIS

Introduction

Titanium and its alloys are of great interest for spatial, chemical, and biomedical industries because of their high resistance to corrosion in air, aqueous and biological media. This property has been associated with the formation of a thin, compact and adherent oxide layer formed on the metal [1–3]. Furthermore, the oxide formed on Ti has shown both a good electrocatalytic [4] and photoelectrochemical activity [5]. Likewise, it has been used as photoanode in cells for solar energy conversion into electrical energy [6], photoelectrocatalytic elimination of pollutants [7], and hydrogen production [8]. The stability and reactivity of the oxide film formed depends on its physico-chemical and semiconductor properties, the latter giving Ti oxide films interesting electronic properties combined with a high resistance of Ti oxide film in aggressive media [9].

Different works have shown that the semiconductor properties of Ti oxide films are a function of the preparation method. Schmidt et al. have found that anodic Ti oxide films show *n*-type semiconductor characteristics caused by a high concentration of oxygen vacancies and presence of Ti^{3+} defects [9], with both oxygen vacancies and Ti^{3+} electronically assumed as donor-like species. The presence of Ti^{3+} and different Ti oxides (i.e., TiO, Ti_2O_3, and TiO_2) have been detected by using the X-ray photoelectron spectroscopy (XPS) technique [10, 11], and other oxides with lower oxidation state (i.e., Ti_3O_5, Ti_4O_7, and Ti_5O_9) have also been reported [12–16]; however, only Ti_3O_5 has been identified using X-ray diffraction [14, 15]. Although

different Ti oxides can be formed during the electroformation of the passive film, the TiO_2 has been reported to be in a greater proportion in all cases.

The Pourbaix diagrams may provide thermodynamic information about the stability region of different species generated through chemical and/or electrochemical reactions in aqueous systems. The well-known Pourbaix diagram for the system Ti-H_2O [17] shows only one predominant species in the whole stability region of water, i.e., TiO_2. For more negative potentials, small zones for Ti_2O_3 and TiO are present. However, the inclusion of more species (soluble species, hydrated species, and oxides with intermediate stoichiometries among others) in the construction of Pourbaix diagram may modify the zones of stability in the Pourbaix diagram. In order to observe the effect of anhydrous and hydrated species in the Pourbaix diagram, Kelsall et al. [18] constructed the Ti-H_2O fraction vs. E diagrams (Fig. 1). The diagram in Fig. 1 takes into account anhydrous oxides with intermediate stoichiometries (Fig. 1a) and hydrated species (Fig. 1b), at 25 °C and pH=12.5. In Fig. 1a, when anhydrous oxides with intermediate stoichiometries are considered, the stability zones of the species are similar to those found in the Ti-H_2O Pourbaix diagram [17]. On the other hand, when hydrated species are considered, Fig. 1b, the stability region of hydrated TiO_2 decreases and is relegated to positive potentials. The zones where TiO and hydrated Ti_2O_3 are thermodynamically stable are increased, and their stability zones are displaced to more positive potentials.

Metikoš-Huković and Ceraj-Cerić [20] studied the formation of oxide films on Ti in different media using

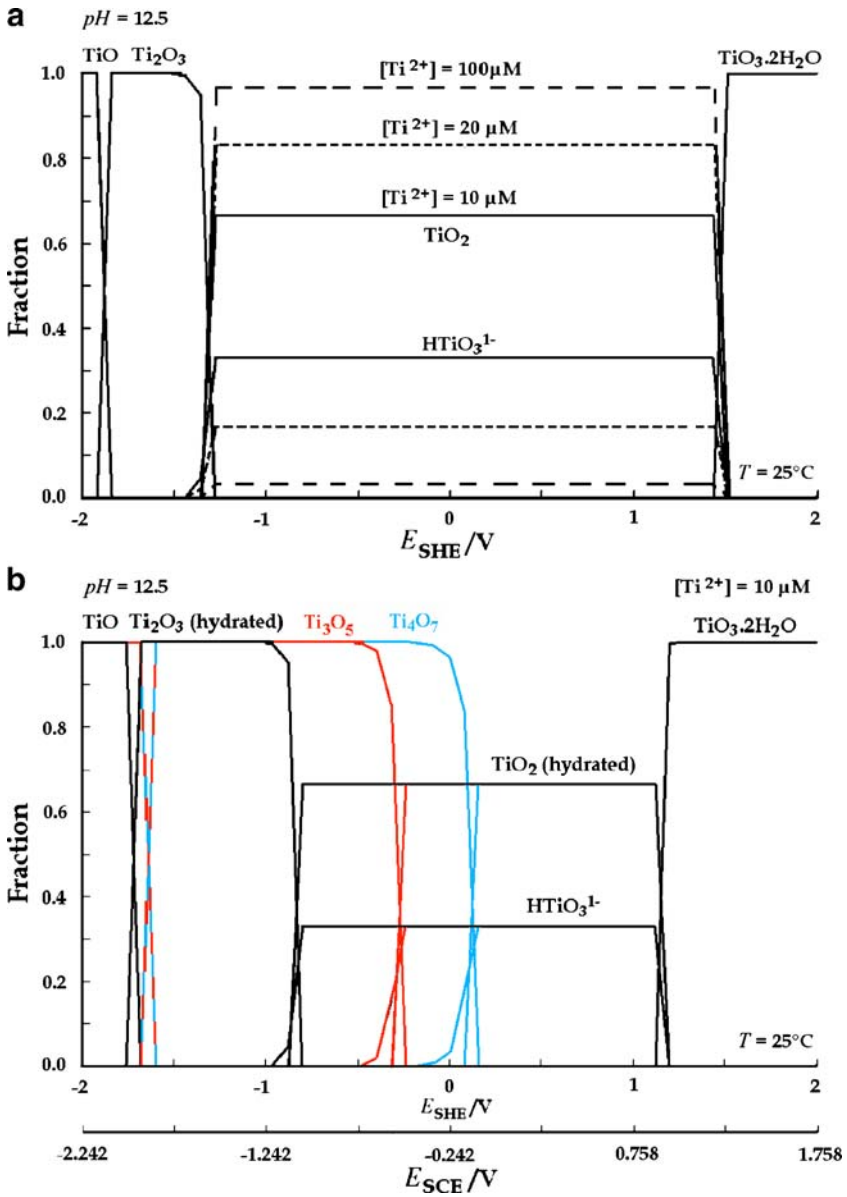

Fig. 1 Fractions diagrams of Ti/H_2O considering oxides with intermediate stoichiometries: **a** Ti-anhydrous species at different [Ti^{2+}] and, **b** Ti-hydrated species at [Ti^{2+}]=10µM. These diagrams were constructed using Medusa chemical equilibrium software [19] and the corresponding equilibrium constants reported by Kelsall [18]

photopolarization. On the basis of their results, they proposed that the oxide film composition varies with the potential, from low to high states of oxidation according to the following model:

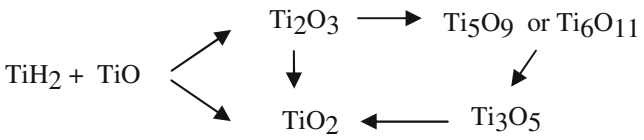

On the other hand, there are also reports concerning with the formation of a thin TiO_3 layer at the surface of the Ti oxide film [21, 22], at potentials where oxygen evolution reaction takes place. A practical application concerning the variable composition potential dependent of the Ti oxide film could be in the design of better materials with specific properties for electrical and photochemical use.

In this work, the changes in composition and structural transformation during the anodic growth of Ti oxide films and its influence on the resistive properties of the film are studied. In the present research, titanium oxides are electrochemically grown employing different strategies in order to detect composition changes of Ti oxides as well as changes in its resistive properties.

Experimental

Materials and equipment

A 99.95% purity Ti rod (Alfa Aesar) embedded in Teflon was used as a working electrode leaving an area of 0.32 cm^2 exposed. Prior to any measurement, the electrode was polished with a silicon carbide emery paper grade 1200, and subsequently was polished with alumina (0.05 μm) using a Buehler Minimet® 1000 automatic polisher until a mirror surface was obtained. Afterwards, the electrode was rinsed with milli-Q water (18.2 MΩ) and placed in an ultrasonic bath for 5 min and rinsed again. Electrochemical tests were performed in a conventional three-electrode cell. A saturated calomel electrode (SCE) coupled to a Luggin capillary was used as reference electrode. All potentials are reported vs. this electrode. A graphite rod was used as a counter-electrode (99.999% Alfa Aesar). The 0.1-M NaOH solution was prepared using milli-Q water (18.2 MΩ) and NaOH in flakes (JT Baker) with 97% purity. Cyclic voltammetry tests were performed in an AUTOLAB potentiostat/galvanostat (PGSTAT 30 model). To determine the open circuit potential (E_{OCP}), chronoamperometry and electrochemical impedance spectroscopy (EIS) studies were carried out in a potentiostat/galvanostat E&GG PAR 283 coupled to a Solartron SI 1260 frequency analyzer for impedance measurements.

Open circuit potential (E_{OCP}) measurement

Measurement of the open circuit potential (E_{OCP}) of the electrode was initiated immediately after the Ti electrode was immersed into the electrolyte, and the E_{OCP} was measured for 1 h with the aim of observing the behavior of the system over time.

Cyclic voltammetry characterization

The electrochemical window of Ti in 0.1 M NaOH solution was determined by a series of cyclic voltammograms starting from the potential measured immediately after immersing the Ti electrode in the solution (−0.77 V) up to different anodic switching potentials ($E_{\lambda a}$=5.42, 4.42, 3.92 V) with a scan rate of 20 mV/s. The influence of $E_{\lambda a}$ on the electrochemical behavior of oxide films was determined by a series of continuous cyclic voltammograms without removing the electrode from the solution. The potential scan started at −0.77 V going up to $E_{\lambda a}$ and returning to the same potential (−0.77 V), and at this potential, the direction of the potential scan was reversed. In the first cycle, $E_{\lambda a}$ is –0.18 V, and for each successive cycle, this value was increased by 0.50 V until reaching an upper limit of 3.92 V in the last cycle. Additional series of voltammograms were recorded in order to evaluate the reduction processes of the anodic film; the cathodic potential limit was −1.75 V for this series.

Electrochemical characterization during the early stages of potentiostatic formation of the oxide film

In order to study the early stages of film electroformation with different formation potentials, E_f, experiments were performed to evaluate changes at 1, 5, 10, 15, and 30 min. Consecutively, cyclic voltammetry was performed in the cathodic direction from E_f to −1.75 V, with a scan rate of 20 mV/s.

Growth and evaluation of Ti oxide films by EIS

Ti oxide films were grown by imposing different formation potentials (E_f) within the range of 0.17 to 2.17 V vs. SCE. In each case, the impedance spectra were obtained every 30 min in 0.1 M NaOH solution until 3 h was completed. The impedance characterization was performed with the following conditions: (a) at the same potential imposed for the film growth, i.e., 0.17, 0.42, 0.67, 0.74, 0.80, 0.92, 1.17, 1.67, and 2.17 V vs. SCE; (b) the amplitude of perturbation on E_f was ±10 mV; and (c) the frequency range was from 100 kHz to 10 mHz.

Results and discussion

Open circuit potential (E_{OCP})

Once the Ti electrode was polished, it was immersed in 0.1 M NaOH, and the variation of E_{OCP} was recorded over the immersion time. The results are shown in Fig. 2. As shown in the figure, there is an increase in the potential of ~170 mV, associated to an oxidation process due to the formation of a passive layer. The passive layer is composed by a mixture of several oxides: TiO, Ti_2O_3, and TiO_2 [10, 11, 20]. After ~1,900 s, the potential remains constant at a value of approximately −0.58 V, where the oxide film formed is stable.

Analysis by cyclic voltammetry

Determination of the electrochemical window by cyclic voltammetry

Figure 3 shows the typical voltammetric behavior of Ti in the NaOH solution. In Fig. 3, the upper limit of the potential scan was varied. Figure 3 a shows a very fast increase of current (P_1) immediately after the potential scan is started in the positive direction. The increase of current is attributed to the oxidation of the Ti surface. After P_1, a current plateau is observed approximately from −0.30 to 0.90 V. At approximately 1.50 V, a small current peak (P_2) is observed, and at more positive potentials, the current density is higher than the current of the plateau. When the potential is close to 3.50 V, there is a considerable increase of current density. The oxidation current increases as $E_{\lambda a}$ becomes more positive (Fig. 3 b, c). At $E_{\lambda a}$, the scan direction is reversed, going into negative direction, and the current decreases sharply following the typical current behavior of oxides formed on valve metals.

The small peak (P_2) during the direct potential scan has been observed in Ti alloys [14, 15] and other valve metals [23]. Peak P_2 has been attributed to different processes such as (a) oxygen evolution [24], (b) rupture and formation of the film [25], and (c) formation of different oxides in the TiO_2 matrix [13]. The considerable current increment for potentials more positive than 4 V may be associated with oxygen evolution; therefore, a potential of 3.92 V is selected as the upper limit for the voltammetric study. The oxide films formed at these potentials are golden and this golden appearance could be due to TiO_3 formation [9, 21, 22] or thin film interference with light. In order to elucidate the processes associated with peak P_2, a voltammetric characterization was performed using different anodic switching potentials ($E_{\lambda a}$).

Influence of $E_{\lambda a}$ on the oxide formed

The influence of the anodic switching potential ($E_{\lambda a}$) in the formation of anodic films was studied by a series of experiments in which the potential scan was initiated at –0.77 V (OCP), and the switching potential was increased 0.50 V in each cycle, being the first $E_{\lambda a}$ −0.18 V and the last $E_{\lambda a}$ 3.92 V. The cycles were performed in a continuous manner without removing the electrode from solution, with ν=20 mV/s. The results of several cycles are shown in Fig. 4. In the first cycle, Fig. 4 (ii) exhibits a sharp peak, P_1, which is attributed to the oxidation of the Ti surface. Upon reaching −0.18 V, the potential scan direction is reversed, and the current density decreases until a value close to zero. At −0.77 V, the potential scan direction is reversed again (Fig. 4 (iii)); now the current density does not increase (because the electrode has already been oxidized) until the previous $E_{\lambda a}$ (−0.18 V) is exceeded, the potential at which the oxidation process continues. The process is similar in the first four cycles (Fig. 4 (ii–v)). In the fifth cycle (Fig. 4 (vi)), the anodic current starts to superimpose with the current measured in the reverse scan of the immediately previous cycle. This current starts to increase at potentials

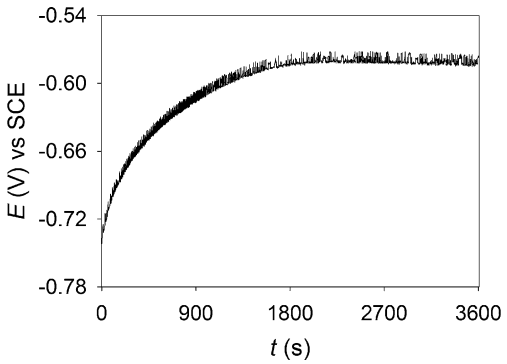

Fig. 2 Variation of open circuit potential (E_{OCP}) of Ti electrode in 0.1 M NaOH

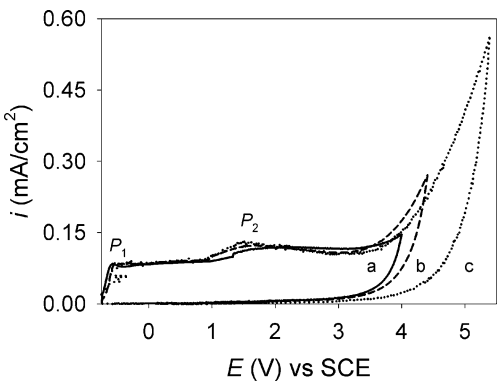

Fig. 3 Cyclic voltammetry curves (ν=20 mV/s) obtained from Ti electrode in 0.1 M NaOH, going to different switching potentials $E_{\lambda a}$ (V vs. SCE), *a* 3.92, *b* 4.42, and *c* 5.42

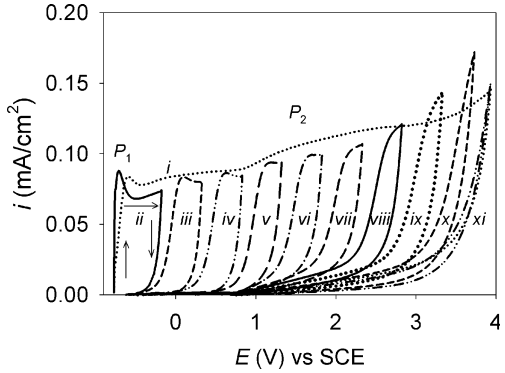

Fig. 4 Cyclic voltammetry curves (v=20 mV/s) obtained from Ti electrode in 0.1 M NaOH, *i* continuous voltammogram throughout the passive region. Several cycles with different $E_{\lambda a}$ (V vs. SCE): *ii* −0.18, *iii* 0.32, *iv* 0.82, *v* 1.32, *vi* 1.82, *vii* 2.32, *viii* 2.82, *ix* 3.32, *x* 3.72, and *xi* 3.92

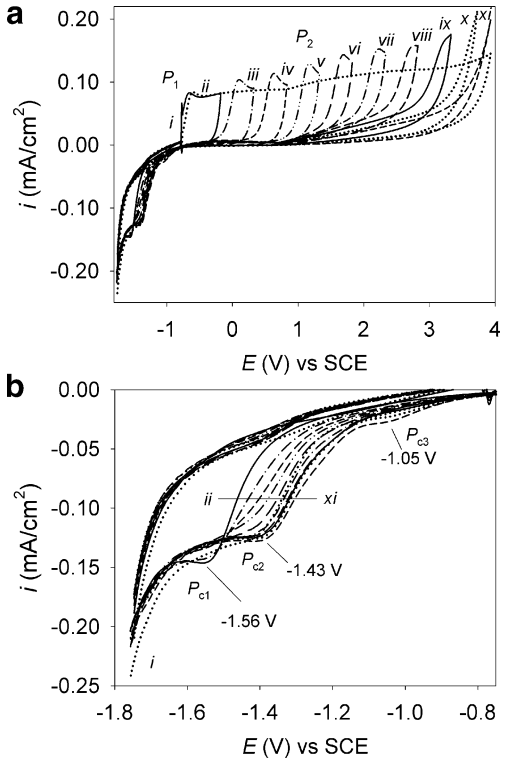

Fig. 5 Cyclic voltammetry curves (v=20 mV/s) obtained from Ti electrode in 0.1 M NaOH. The lower potential limit=−1.75 V, the upper potential limit is varied. *i* Continuous voltammogram throughout the passive region. Several cycles with different $E_{\lambda a}$ (V vs. SCE): *ii* −0.18, *iii* 0.32, *iv* 0.82, *v* 1.32, *vi* 1.82, *vii* 2.32, *viii* 2.82, *ix* 3.32, *x* 3.72, and *xi* 3.92. **a** Whole scanned potential window and, **b** zoom of cathodic zone

greater than 0.90 V, after which the slope of the curve changes at the potential where the previous cycle has been completed. Figure 4 also shows that currents obtained only overcome the currents of the continuous cycle (Fig. 4(i); in the last three cycles, Fig. 4 (ix–xi)), possibly due to oxygen evolution.

Peláez-Abellan et al. [22] carried out a similar voltammetric study on Ti, in phosphates (Na_2HPO_4/NaH_2PO_4) neutral medium, with $E_{\lambda a}$ variations of 1.00 V. The results presented by Peláez-Abellan et al. show similar behavior regarding oxygen evolution on the electrode. On the other hand, Oliveira et al. [14] found that Ti oxides, in acid medium of H_3PO_4/NaH_2PO_4, have electrocatalytic properties for O_2 evolution. According to the paper of Oliveira et al., the greater the number of cycles, the greater is the current associated with water oxidation. In order to differentiate the processes occurring within the potential region of study, the influence of $E_{\lambda a}$ on the associated reduction processes was evaluated.

$E_{\lambda a}$ influence on the reduction processes of Ti oxide film

Several voltammetric cycles were used in order to evaluate reduction processes of oxides formed during direct potential scans using different $E_{\lambda a}$ (similar as in the Fig. 4); for these experiments, the lower potential limit was kept constant at a more negative potential than in Fig. 3 in all cycles, i.e., −1.75 V. As a first test, a complete cycle between −1.75 and 3.92 V was performed. Figure 5a(i) shows the behavior of this experiment. The voltammogram in Fig. 5 is similar to that shown in Fig. 3; however, a small peak (P_{c2}) at −1.43 V associated to the reduction of Ti oxide film is detected. In this potential region, the cathodic current has a contribution from hydrogen evolution (Fig. 5b(i)).

After this experiment, different cycles were accomplished with the electrode surface freshly polished again. Firstly, a scan in the positive direction was initiated at –0.77 V (Fig. 5a(ii)), producing a sharp peak P_1 attributed to Ti oxidation. At −0.18 V, the potential scan direction was reversed and the current density now decreased close to zero. When the scan continued for potentials more negative than −0.77 V, a cathodic peak P_{c1} appears (Fig. 5b(ii)); after this peak, the cathodic current increases due to the hydrogen evolution reaction. Following the second consecutive cycle (Fig. 5a(iii)) from -1.75 V and going to positive direction, the current density decreases close to zero, and current density does not present positive values until the previous $E_{\lambda a}$ (−0.18 V) is overcome. For potentials greater than −0.18 V, the oxidation process continues and current density increases again (Fig. 5a(iii)). In Fig. 5(iii–xi), the oxidation current densities overcome the value achieved in the first cycle (Fig. 5a(i)). In Fig. 4, the lower limit was −0.77 V and the oxidation current densities overcome the value achieved in the first cycle only in the last three cycles (Fig. 4(ix–xi)). The superposition currents generated after the fourth scan, in Fig. 4(vi–xi), are smaller than those found in Fig. 5(vi–xi).

Figure 5b shows the cathodic currents measured during the reverse scan after reaching different $E_{\lambda a}$, and three

cathodic peaks (P_{c1}, P_{c2}, and P_{c3}) which depend on $E_{\lambda a}$ are found. The first peak, P_{c1}, formed at −1.56 V appears when $E_{\lambda a}$ is between −0.18 and 0.32 V (Fig. 5b(ii–iii)). For more positive $E_{\lambda a}$, a second peak, P_{c2}, begins to form at −1.43 V (Fig. 5b(iv–xi)). The third peak, P_{c3}, at –1.05 V appears only when $E_{\lambda a}$ reaches a value of 3.92 V (Fig. 5b(xi)), the potential at which oxygen evolution reaction takes place. The presence of P_{c1}, P_{c2}, and P_{c3} peaks indicates that during the anodic film formation on Ti, in the potential range from −0.77 to 3.92 V, different structural transformations occur within the film and depend on $E_{\lambda a}$.

The voltammetric characterization of titanium oxide films shows the oxide dependence of the potential used for its formation. However, it is important to mention that voltammetric studies always involve a competition between the formation rate of the species at the interface and the electrode polarization rate; therefore, some oxidation processes would not be clearly identified. On the contrary, when studies are potentiostatically performed, energetic conditions are imposed to the electrode and the evolution of chemical species formed on the surface can be monitored over time. For this reason, the following section deals with the electrochemical characterization of Ti oxides during the early stages of potentiostatically formed films.

Electrochemical evaluation during early stages in oxide formation

The potentiostatic growth of Ti oxide film was carried out at 1, 5, 10, 15, and 30 min, using different formation potentials, E_f, −0.18, 1.82, and 3.92 V; immediately after the potential step, a cyclic voltammetry was performed in the cathodic direction v=20 mV/s, from E_f to −1.75 V. Figure 6 shows the voltammograms obtained following this program. The film grown for 1 min at E_f of −0.18 V presents a reduction peak at −1.56 V (Fig. 6a), and it slightly displaces towards less negative potentials as the growth time increases until reaching −1.53 V for 30 min of growth. In the films grown for 1 min at the other two E_f (1.82 and 3.92 V; Fig. 6b, c), a reduction peak appears at −1.56 V, as the time of growth is increased, e.g., for t=30 min, the peak potentials are −1.50 and −1.43 V for E_f of 1.82 and 3.92 V, respectively.

As it was mentioned before, even when the passive film formed on Ti is a mix of different oxides, from a macroscopic point of view, it behaves like one oxide. Then, the relation of the oxides presented in the film will rule its properties and its electrochemical behavior. In Fig. 6, the reduction peak of films grown with E_f, –0.18, 1.82, and 3.92 V, at the very initial stages of growth is approximately the same; this may indicate that the proportions of the oxides within the film are similar at the very initial stages. However, when the growth time is increased, the reduction peak appears at more positive values, and this may indicate a variation in the proportion of the different oxides within the film. This suggests that film formation starts from the same oxide film, regardless of E_f, but its structure is changing as E_f and the growth time is modified. Based on the above results, it can be proposed that Ti oxide films are not formed by direct formation of TiO_2, but during intermediate stages of oxidation, which may be associated with the formation of TiO and Ti_2O_3. This means that the film would be made up of a mixture of these three oxides. On the basis of this hypothesis, the following mechanism of film formation can be proposed.

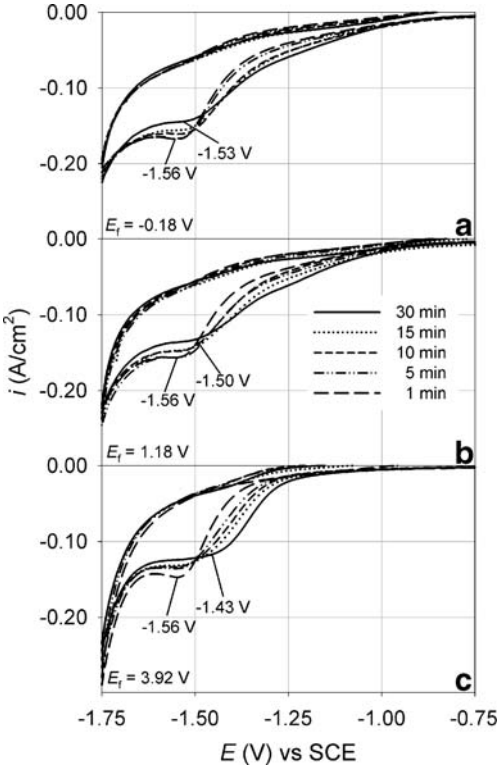

Fig. 6 Cyclic voltammograms (v=20 mV/s) of titanium oxide films formed in 0.1 M NaOH by applying different E_f (V vs. SCE): **a** −0.18, **b** 1.82, and **c** 3.92, using different growth times: 1, 5, 10, 15, and 30 min, indicated in the figure

Firstly, a primitive oxide film composed of a mixed of oxides is formed due to the reaction of Ti surface with air (Eqs. 1–3) or H_2O (Eqs. 4 and 5) when in contact with solution [17]; these chemical reactions are responsible for the E_{OCP} variation over t (Fig. 2). Even when the proportion of the oxides formed at E_{OCP} have been reported to favor towards TiO_2, the proportion of the other oxides (Ti_2O_3 and TiO) may be important, and this is also shown in the chemical species fraction diagram of Fig. 1.

$$2Ti + O_2 \rightarrow 2TiO \quad (1)$$

$$2\mathrm{TiO} + \frac{1}{2}\mathrm{O_2} \rightarrow \mathrm{Ti_2O_3} \quad (2)$$

$$\mathrm{Ti_2O_3} + \frac{1}{2}\mathrm{O_2} \rightarrow 2\mathrm{TiO_2} \quad (3)$$

The proportion of Ti oxides can be changed by imposing anodic potentials, causing the oxidation of the oxides with low oxidation state (Eqs. 4 and 5).

$$2\mathrm{TiO} + \mathrm{H_2O} \rightarrow \mathrm{Ti_2O_3} + 2\mathrm{H^+} + 2\mathrm{e^-} \quad (4)$$

$$\mathrm{Ti_2O_3} + \mathrm{H_2O} \rightarrow 2\mathrm{TiO_2} + 2\mathrm{H^+} + 2\mathrm{e^-} \quad (5)$$

As can be inferred from the voltammetric study, the percentage of TiO and Ti_2O_3 transformation depends on the potential and time of film formation, allowing the formation of different mixtures of these oxides. The change in the oxide proportion provokes changes in the properties of the film. Even though other oxides such as Ti_3O_5, Ti_4O_7 [18], Ti_5O_9, and Ti_6O_{11} [20] have been proposed as part of the Ti oxide film, XPS results [10, 11] have shown that these films consist of a mixture of TiO (in contact with Ti substrate), Ti_2O_3, and TiO_2 in the most external part of the film, so other oxides may be considered as mixtures of Ti_2O_3 and TiO_2, formed due to enrichment of TiO_2 in the film ($Ti_2O_3 \cdot mTiO_2$, $1 \leq m \leq 4$). In order to evaluate the resistive properties of the film composed of different Ti oxides, the EIS was used.

Growth and evaluation of anodic films by EIS and chronoamperometry

The Ti oxide films were potentiostatically grown using nine different formation potentials (E_f=0.17, 0.42, 0.67, 0.74, 0.80, 0.92, 1.17, 1.67, and 2.17 V vs. SCE) located in the potential zone where structure transformations take place. The chronoamperograms obtained during the potentiostatic growth with different E_f are shown in Fig. 7. The pseudo-steady-state current density i_{ss}, (indicated as a dotted black line in Fig. 7) after 3 h, presents two cases: (a) For E_f< 0.80 V, current densities are low and increase with E_f, and (b) for E_f>0.92 V, currents are higher than case (a) and are almost independent from E_f (Fig. 7). The slow increase in almost two orders of magnitude of i_{ss} in zone I shows the evolution of resistive properties of the oxide film with E_f. In zone II, i_{ss} is constant. The progressive change in the resistive properties of the oxide film can be related to the progressive evolution in the proportion of Ti oxides inside the film, while for greater potentials, an enrichment of TiO_2 is achieved and the properties of the film do not greatly change.

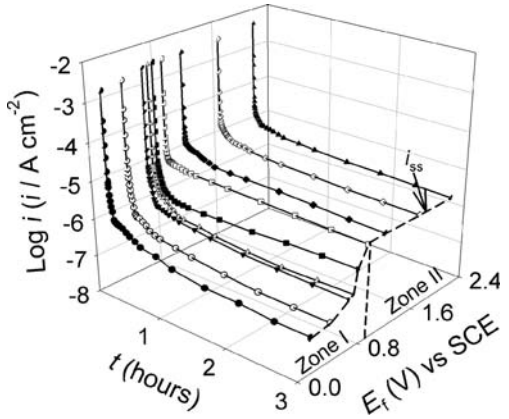

Fig. 7 Variation of Log i vs. t obtained from the potentiostatic formation of Ti oxide films in 0.1 M NaOH using different formation potentials, E_f

The impedance characterization was carried out using ±10 mV perturbation signal, within a frequency range from 100 kHz to 10 mHz. The Nyquist spectra of the Ti oxide film formed with different growth times are shown in Fig. 8. In the figure, the real and imaginary components of impedance (Z_{re}, Z_{im}) show increase in their values for the spectra with t<2 h; however, the magnitudes of Z_{re} and Z_{im} are very similar for the spectra with $t \geq 2$ h, and this indicates that after 2 h, the film composition does not change very much, reflected in the impedance diagrams which are now independent of time (Fig. 8).

Figure 9a–f shows Nyquist and Bode plots obtained from the oxide films formed potentiostatically during 2 h and different E_f. In this figure, two tendencies are found which depend on E_f. For E_f<0.92 V (Fig. 9a), Nyquist spectra have two loops: the first one appears at high frequencies, and this loop does not depend on E_f; the second loop shows a strong dependence on E_f, and the imaginary component decreases with the increase of E_f until the spectrum finally acquires the appearance of a flattened semicircle. In Bode plots (Fig. 9b, c), the phenomenon is reflected as a decrease in the phase angle at low

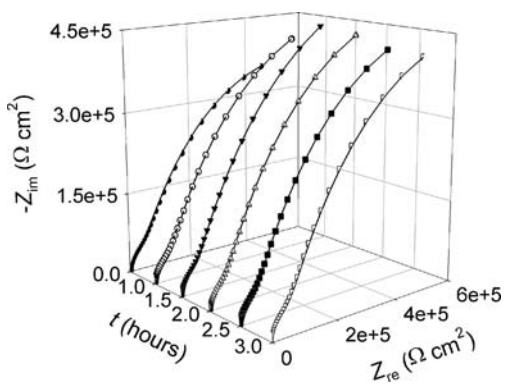

Fig. 8 EIS spectra of Ti oxide film formed in 0.1 M NaOH at E_f= 0.67 V, with different growth times

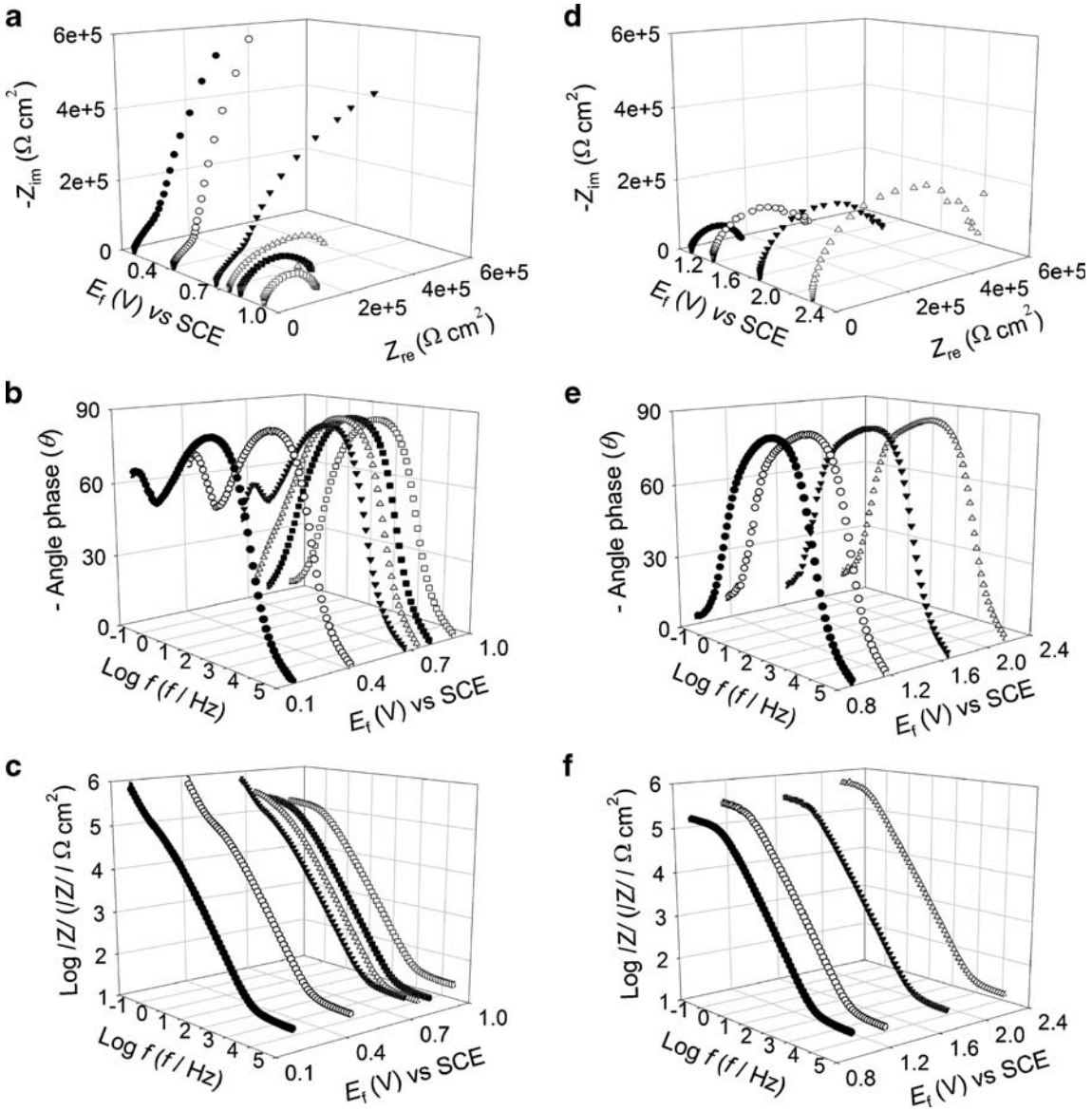

Fig. 9 Nyquist and Bode plots obtained from Ti oxide films formed in 0.1 M NaOH during 2.0 h, using different formation potentials, E_f. **a, b, c** Films formed for E_f<0.92 V; **c, d, e** Films formed for $E_f \geq 0.92$ V

frequencies, and a change in the second slope, formed at low frequencies. For $E_f \geq 0.92$ V (Fig. 9d), Nyquist plots show that as the E_f increases the real and imaginary components increase, in the Bode plots, the phase angle remains practically constant (Fig. 9e), but the impedance magnitude also increases with the potential (Fig. 9f). To obtain quantitative information from these plots, an equivalent circuit fitted to the entire range of frequencies was employed.

Equivalent circuit fit and analysis of impedance spectra

The analysis of the impedance spectra using equivalent electric circuits (eec) can be a useful tool to describe the impedance response of Ti oxide films. With this purpose, the eec in Fig. 10a was employed, and this circuit allows a good fit ($\chi^2 \sim 10^{-4}$) to experimental EIS diagrams, as it is shown for experimental Nyquist and Bode plots (Fig. 10b, c). R_S is the solution resistance, and R_C and CPE_c are the resistance and the constant phase element associated with the mix of different Ti oxides. The impedance of this element is defined by $Z_{CPE} = 1/[(j\omega)^{n_c} Q_c]$, n_c is a constant which compensates for the non-homogeneity of the system, and Q_c is the capacitance associated with the oxide film. R_p and CPE_p are the resistance and the constant phase element associated to an outer porous layer formed by hydrated Ti oxides; the impedance is defined by $Z_{CPEp} = 1/\left[(j\omega)^{n_p} Q_p\right]$, where n_p and Q_p are analogously defined.

Figure 11a shows the values of R_C obtained from the fit of EIS spectra with the circuit in Fig. 10a. The values of R_C

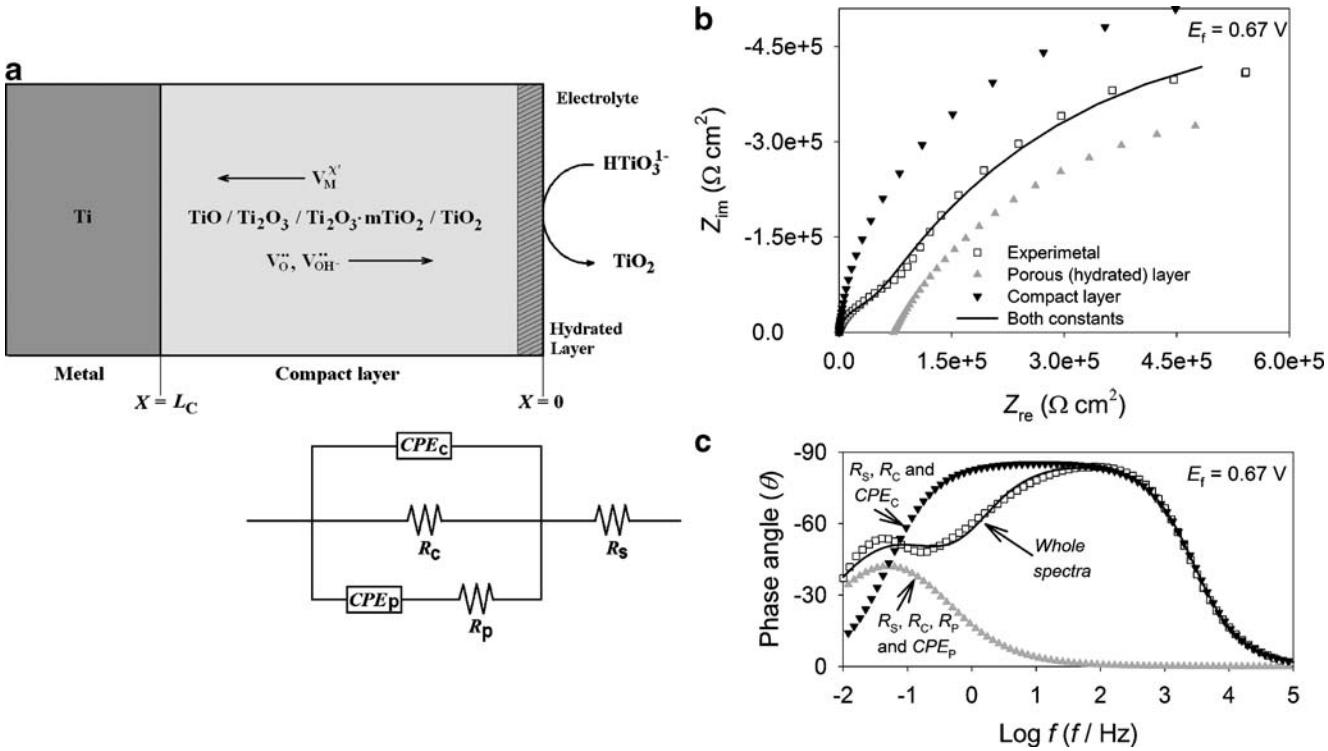

Fig. 10 **a**–**c** Electric equivalent circuit (*eec*) used for fitting process of the experimental impedance spectra from Ti oxide films. The figure shows the different processes on the interfase Ti/film/0.1 M NaOH associated to the electric elements of the eec

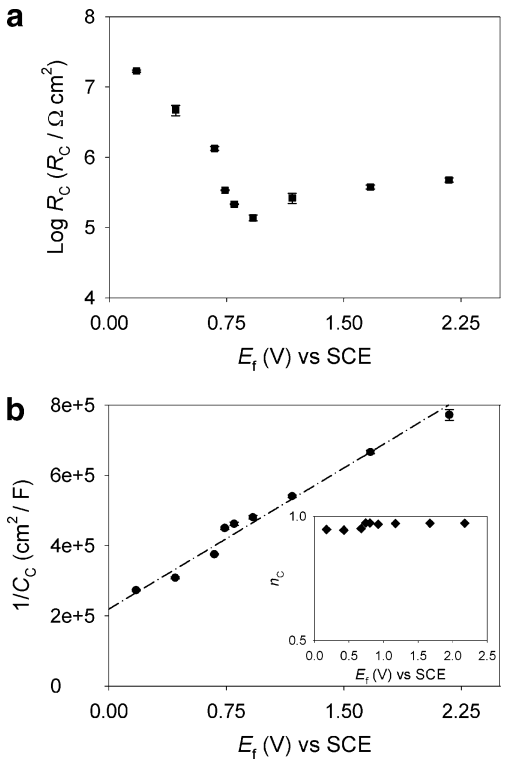

Fig. 11 Variation of the circuit elements of Fig. 10 obtained from the fit of Ti oxide films impedance spectra. **a** Log R_C and **b** $1/C_C$; the *inset* shows n_C

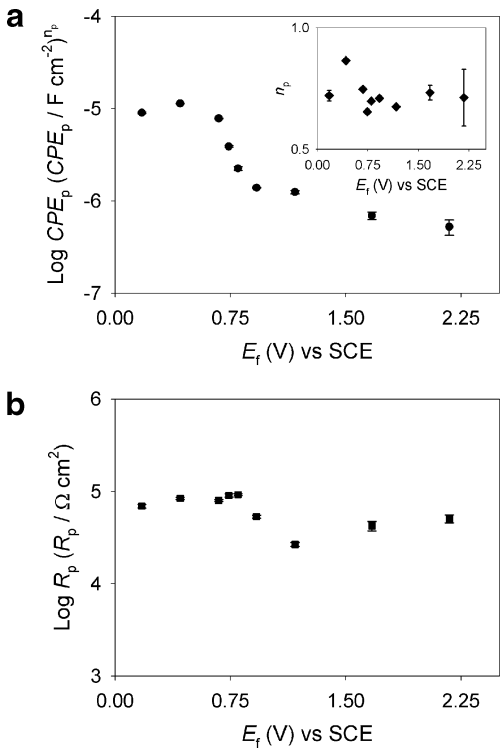

Fig. 12 Variation of the circuit elements of Fig. 10 obtained from the fit of the Ti oxide films impedance spectra. **a** $1/CPE_p$; the *inset* shows n_C and **b** Log R_p

are plotted vs. E_f, and two tendencies with E_f can be observed. The value of R_C decreases in two orders of magnitude for E_f<0.924 V, and this may be associated with the change in composition of Ti oxide films until TiO_2 dominates the electric response $E_f \geq 0.924$ V. The inset of Fig. 11b shows the dependence of n_c with E_f. Since n_c acquires values within the range of 0.95 to 0.98, the behavior of this constant phase element is assumed to be very similar to an ideal capacitor, thereby $Q_C \approx C_C$, where C_C is the capacitance of the oxide layer. Although the voltammetric characterization indicates structure transformations within the oxide film, Fig. 11b shows a linear relationship of $1/C_C$ with E_f, and this behavior is typically reported for oxide films grown on valve metals [26, 27]. The oxide film thickness (L_c) is related with C_C through Eq. 6.

$$\frac{1}{C_C} = \frac{L_C}{\varepsilon_r \varepsilon_o} \tag{6}$$

Where L_C is the film thickness, ε_o is the vacuum permittivity (8.8542×10^{-12} F/m), and ε_r is relative permittivity of the oxide.

The oxide film thickness in turn can be related to E_f through Eq. 7 [28], where a is the anodizing ratio of the oxide film, E_f is the formation potential, and b is the film thickness at E_f=0 V.

$$L_C = aE_f + b \tag{7}$$

By combining Eqs. 6 and 7, the relationship between $1/C_C$ and the formation potential, E_f, is obtained (Eq. 8):

$$\frac{1}{C_C} = \frac{a}{\varepsilon_r \varepsilon_0}\left[E_f + \frac{b}{a}\right] \tag{8}$$

Prusi et al. [28] studied the growth kinetics for potentiostatically formed oxide films under similar conditions (Ti/0.1 M NaOH), within the potential range between 0 and 90 V. The film thickness was calculated using in situ ellipsometry. With this technique, Prusi et al. calculated the anodizing ratio, a=2.38 nm/V.

The linear behavior of $1/C_C$ with E_f and a=2.38 nm/V allows determining the value of ε_r (~38) by means of Eq. 8. The value of ε_r corresponds to oxide film composed of different Ti oxides, where the mix as a whole behaves as one electric layer.

Figure 12a presents the values of CPE_p associated with the capacitance of the outer layer, formed by hydrated Ti oxides. The CPE_p behavior with E_f can be related with the change in the oxide film composition by taking into account that the composition of the inner layer depends on E_f. The capacitance of the outer layer is sensitive to the structure and composition of the oxide film and therefore there is change in CPE_p behavior. The variation of R_p with E_f presents in a similar way a variation related to the oxide film composition in the outer layer.

Conclusions

The voltammetric study of the Ti electrode in the 0.1-M NaOH solution indicates the presence of different Ti oxides formed during the anodic growth. The typical voltammograms of Ti in 0.1 M NaOH show several peaks; the anodic peak P_2 at a potential of 1.50 V can be associated with the oxidation of TiO and Ti_2O_3 to TiO_2 within the film. It was found that peaks (P_{c1}, P_{c2}, and P_{c3}) depend on the anodic switching potential ($E_{\lambda a}$).The peaks P_{c1} and P_{c2} can be attributed to the reduction of Ti_2O_3 and TiO_2. Peak P_{c3} can be associated to the reduction of TiO_3, or to the reduction of hydrogen peroxide formed at high anodic potentials (3.92 V).

The evaluation of the resistive properties of Ti oxide films determined by EIS shows that despite the chemical transformations within the film, there is a linear dependence of $1/C_C$ with E_f, as it is typically reported for valve metals. The linear behavior of $1/C_C$ with E_f and assuming a= 2.38 nm/V allowed determining the value of ε_r (~38). The value of ε_r corresponds to oxide film composed by different Ti oxides, where the mix as a whole behaves as one electric layer.

Acknowledgments This work has been carried out in the frame of the projects COLCIENCIAS (Project 1102-332-18533) and CONACYT (Project SEP-2004-C01-47162). P. Acevedo-Peña thanks the Universidad Industrial de Santander for the master scholarship and the financial support through the "Program for Mobility of Researchers 2007-VIE". G. Vázquez thanks the financial support of CONACYT for the postdoctoral grant.

References

1. Oliveira NTC, Biaggio SR, Piazza S, Sunseri C, Di Quarto F (2004) Electrochim Acta 49:4563. doi:10.1016/j.electacta.2004.04.042
2. Kelly RG, Scully JR, Shoesmith DW, Buchheit RG (2002) Electrochemical techniques in corrosion science and engineering. Marcel Dekker, New York
3. Pan J, Thierry D, Leygraf C (1996) Electrochim Acta 41:1143. doi:10.1016/0013-4686(95)00465-3
4. Roh B, Macdonald DD (2007) Russian. J Electrochem Soc 43:125
5. Kale SS, Mane RM, Ganesh T, Pawar BN, Sung-Hwan H (2009) Curr Appl Phys 9:384. doi:10.1016/j.cap.2008.03.016
6. Xie Y (2006) Electrochim Acta 51:3399. doi:10.1016/j.electacta.2005.10.003

7. Palombari R, Ranchella M, Rol C, Sebastiani GV (2002) Sol Energy Mater Sol Cells 71:359. doi:10.1016/S0927-0248(01)00093-9
8. Raja KS, Mahajan VK, Misra M (2006) J Power Sources 159:1258. doi:10.1016/j.jpowsour.2005.12.036
9. Schmidt AM, Azambuja DS, Martini EMA (2006) Corros Sci 48:2901. doi:10.1016/j.corsci.2005.10.013
10. Ibrahim MAM, Pongkao D, Yoshimura M (2002) J Solid State Electrochem 6:341. doi:10.1007/s100080100229
11. Xia Z, Nanjo H, Aizawa T, Kanakubo M, Fujimura M, Onagawa J (2007) Surf Sci 601:5133. doi:10.1016/j.susc.2007.04.211
12. De Pauli CP, Giordano MC, Zerbino JO (1983) Electrochim Acta 28:1781. doi:10.1016/0013-4686(83)87014-5
13. Camara OR, de Pauli CP, Giordano MC (1984) Electrochim Acta 29:1111. doi:10.1016/0013-4686(84)87163-7
14. Oliveira EM, Marino CEB, Biaggio SR, Rocha-Filho RC (2000) J Electrochem Soc 2:254
15. Marino CEB, de Oliveira EM, Rocha-Filho RC, Biaggio S (2001) Corros Sci 43:1465. doi:10.1016/S0010-938X(00)00162-1
16. Huang YZ, Blackwood DJ (2005) Electrochim Acta 51:1099. doi:10.1016/j.electacta.2005.05.051
17. Pourbaix M (1974) Atlas of electrochemical equilibria in aqueous solutions. NACE, Houston
18. Kelsall GH, Robbins DJ (1990) J Electroanal Chem 283:135. doi:10.1016/0022-0728(90) 87385-W
19. Medusa (chemical equilibrium software) (2004). Royal Institute of Technology (KTH), Stockholm. http://www.kemi.kth.se/medusa. Accessed 15 Oct 2008
20. Metikoš-Huković M, Ceraj-Cerić M (1985) Surf Technol 24:273. doi:10.1016/0376-4583(85)90077-9
21. Azumi K, Seo M (2001) Corros Sci 43:533. doi:10.1016/S0010-938X(00)00105-0
22. Peláez-Abellán E, Rocha-Sousa L, Müller WD, Guastaldi AC (2007) Corros Sci 49:1645. doi:10.1016/j.corsci.2006.08.010
23. Biaggio S, Bocchi N, Rocha-Filho RC, Varela FE (1997) J Braz Chem Soc 8:615
24. Di Quarto F, Piazza S, Sunrei C (1990) Electrochim Acta 35:99. doi:10.1016/0013-4686(90)85045-O
25. Macdonald DD (1992) J Electrochem Soc 139:3434. doi:10.1149/1.2069096
26. Vázquez G, González I (2007) J Electrochem Soc 154:C702. doi:10.1149/1.2780870
27. Sikora E, Sikora J, MacDonald DD (1996) Electrochim Acta 41:783. doi:10.1016/0013-4686(95)00312-6
28. Prusi A, Arsov L, Haran B, Popov BN (2002) J Electrochem Soc 149:B491. doi:10.1149/1.1510134